

Vertical distribution of snow cover and its relation to temperature over the Manasi River Basin of Tianshan Mountains, Northwest China

ZHENG Wenlong^{1,2}, *DU Jinkang^{1,2}, ZHOU Xiaobing³, SONG Mingming^{1,2},
BIAN Guodong^{1,2}, XIE Shunping^{1,2}, FENG Xuezhi^{1,2}

1. Department of Geographic Information Science, Nanjing University, Nanjing 210023, China;

2. Jiangsu Center for Collaborative Innovation in Geographical Information Resource Development and Application, Nanjing 210023, China;

3. Department of Geophysical Engineering, Montana Tech of the University of Montana, Butte, MT 59701, USA

Abstract: How snow cover changes in response to climate change at different elevations within a mountainous basin is a less investigated question. In this study we focused on the vertical distribution of snow cover and its relation to elevation and temperature within different elevation zones of distinct climatology, taking the mountainous Manasi River Basin of Xinjiang, Northwest China as a case study. Data sources include MODIS 8-day snow product, MODIS land surface temperature (LST) data from 2001 to 2014, and *in situ* temperature data observed at three hydrological stations from 2001 to 2012. The results show that: (1) the vertical distribution of snow areal extent (SAE) is sensitive to elevation in low (<2100 m) and high altitude (>3200 m) regions and shows four different seasonal patterns, each pattern is well correspondent to the variation of temperature. (2) The correlation between vertical changes of the SAE and temperature is significant in all seasons except for winter. (3) The correlation between annual changes of the SAE and temperature decreases with increasing elevation, the negative correlation is significant in area below 4000 m. (4) The snow cover days (SCDs) and its long-term change show visible differences in different altitude range. (5) The long-term increasing trend of SCDs and decreasing trend of winter temperature have a strong vertical relation with elevation below 3600 m. The decreasing trend of SCDs is attributed to the increasing trend of summer temperature in the area above 3600 m.

Keywords: snow cover; vertical distribution; temperature inversion; Manasi River; correlation analysis

1 Introduction

Snow covers an enormous portion of the earth's surface and is very dynamic. Understanding its change and characteristics is imperative to climate change, weather forecasting, and water resource variation and redistribution (Barnett *et al.*, 1989; Brown and Robinson, 2011). In

Received: 2016-03-17 **Accepted:** 2016-06-29

Foundation: National Natural Science Foundation of China, No.41271353

Author: Zheng Wenlong, Master, specialized in snow cover change of remote sensing. E-mail: 380276692@qq.com

***Corresponding author:** Du Jinkang, PhD, E-mail: njudjk@163.com

the Northern Hemisphere the average monthly snow area extent accounts for 7% to 40% during an annual cycle, making snow cover the most variable surface feature of the earth (Hall, 1988). The remote arid alpine regions within Tianshan mountain range in Northwest China are characterized by large elevation gradients, resulting in significant variability of precipitation in different elevation zones. For many watersheds in that region, meltwater is an important source for the various water consuming sectors, especially agricultural irrigation (Feng *et al.*, 2000). Snowpack plays a special role in the water resource storage and regulation within the arid region. Detailed snow cover information is an important input to most snowmelt runoff simulation and forecasting modeling. Precise monitoring of snow cover recession in spring can provide important information for the local water department to efficiently manage water resources and floods. However, meteorological stations for snow cover monitoring are scarce and unevenly distributed because of inaccessibility, and snow process is poorly understood in these remote areas.

Optical remote sensing technology provides an alternative approach for acquiring long-term snow cover information over a large area. Since the Moderate Resolution Imaging Spectroradiometer (MODIS) sensor carried on Terra and Aqua satellites was put into service, the MODIS snow products have been used in snow monitoring and climatic and hydrologic studies over a wide range of locations and periods (She *et al.*, 2015; Spiess *et al.*, 2015; Tahir *et al.*, 2015; Yang *et al.*, 2012). Dietz *et al.* (2015) have developed global snowpack products for studying status and dynamics of the planetary snow cover extent using snow cover daily products of MODIS/Terra (MOD10A1) and MODIS/Aqua (MYD10A1). Jin *et al.* (2015) used the 8-day composite MODIS snow data to analyze the spatio-temporal variations of snow cover on the Loess Plateau and found that the monthly snow cover was strongly teleconnected to the Siberian High Central Intensity (SHCI) but not so to the El Niño Southern Oscillation (ENSO). Marchane *et al.* (2015) applied the MODIS daily snow data to characterize the inter-annual variability of the snow cover area in the Atlas Mountains (Morocco) during 2000–2013 after assessing its accuracy over seven catchments. Tang *et al.* (2013) analyzed the characteristics of spatio-temporal variations of snow cover and their association with *in situ* air temperature in the Tibetan Plateau and found that snow cover accumulation and ablation varied in different elevation zones and snow cover mainly exists within mountainous area. Wang *et al.* (2014) developed a new multiday retrospective cloud-removal approach for MODIS daily snow data to reduce cloud contamination and then analyzed the spatio-temporal variations of snow cover in the Xiao Hinggan Mountains in Northeast China. Their results showed that the snow cover in the watershed increased in recent years, showing a minimum in 2002 and a maximum in 2010.

Snow cover variation has strong connections with climate factors such as land surface temperature and precipitation (Liu *et al.*, 2014; Mishra *et al.*, 2013; Szczypta *et al.*, 2015). Wang *et al.* (2015) examined the response of snow cover to changes in temperature and precipitation over the Tibetan Plateau from 2003 to 2010 using the observation data at meteorological stations, they found that the increase of temperature (0.09°C/year) and precipitation (0.26 mm/year) has a considerable influence on the increasing trend of maximum snow cover area and decreasing trend of persistent snow cover area. Bavay *et al.* (2013) studied the climate change impact on snow cover and runoff in the high alpine catchments of eastern Switzerland based on model simulations. Their results indicated that the impact of climate change on snow cover and runoff is closely related to elevation and size of catchments. Liu

et al. (2007) investigated the impact of air temperature and precipitation on snow cover change in different seasons from 2005 to 2006 over the Dongkemadi River Basin in the source regions of the Yangtze River. They concluded that snowfall during October and November contributes significantly to snow cover variation, while temperature is the principal impact factor during the warm season (May to September) and there is no significant correlation between snow cover and precipitation. However, most of the previous studies on the correlation between snow cover variation and climate factors are based mainly on a linear temporal analysis using *in situ* point data. The MODIS land surface temperature (LST) product can provide a long-term series of temperature distribution with the accuracy better than 1 K (Wan, 2008). Its accuracy validation has been carried out over a widely distributed locations and time periods (Bosilovich, 2006; Coll *et al.*, 2009; Hulley and Hook, 2009; Wan, 2008). But few studies have used the MODIS LST data to explore the spatio-temporal correlation between snow cover and temperature change (Bi *et al.*, 2015).

Vertical variation of snow cover is important in understanding snow accumulation and decay, especially in topographically complex montane terrains. Vertical variation of snow cover has to be considered in snowmelt runoff modeling and assessment of climate change impact on snow cover. However, few spatial analyses of snow cover have included the vertical dimension, analyzing snow cover change within different elevation zones is the most frequently adopted way to explore the vertical variation of snow cover (Tang *et al.*, 2013; Bi *et al.*, 2015)

In this study we focused on the vertical distribution of snow cover and its relation to elevation and temperature for the mountainous Manasi River Basin of Xinjiang. A refined zonation analysis was adopted to divide the whole elevation range into a series of belts to explore how snow cover and temperature change in those refined belts of different elevations. The other purpose of this study is to evaluate the validity of the MODIS 8-day snow data and MODIS LST data.

2 Study area

The Manasi River Basin (43°05'N–44°10'N and 85°00'E–86°20'E) is located in the hinterland of the Eurasian continent, with a total area of 5156 km². It is the fourth biggest irrigation district in Northwest China. The river originates in the northern slope of the Tianshan Mountains, and it is the longest (about 400 km) inland river in the Junggar Basin. The climate of the watershed is temperate continental arid. The topography of the basin is complex, resulting in various vertical zones with distinct climatology. The annual precipitation in the stream source area is 600–700 mm. It decreases to 100–200 mm in the piedmont plain. The upstream with elevation above 3600 m is covered with a contemporary glacier of 608.25 km². Ice melt water is an important water resource, accounting for 34.6% of the total runoff (Feng *et al.*, 2000). Precipitation is abundant within the elevation zone between 1500 m and 3600 m, which is the main flow-generation zone and the main recharge source of the river. From the elevation of 1500 m down to the basin exit at the Hongshanzui (HSZ) hydrological station is the runoff transport area. The area outside the mountain is the runoff dissipation zone. In this study, we focus on the recharge and streamflow transportation area. The study area is thus the portion above the Hongshanzui (HSZ) hydrological station, as is shown in Figure 1. The background is elevation distribution. The four hydrological stations at the lower part of the

basin are also shown: Meiyao (MY), Kensiwate (KSWT), Qingshuihezi (QSHZ), and Hongshanzui (HSZ).

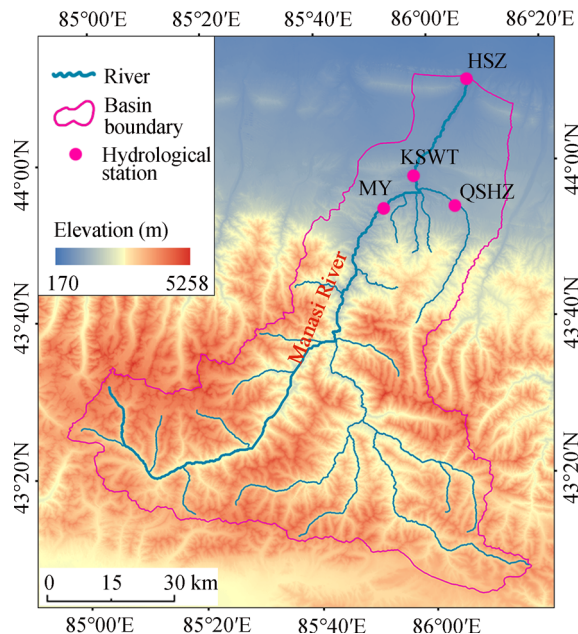


Figure 1 The boundary, river network, hydrological stations and elevation distribution of the study area

3 Data and methods

3.1 Data

(1) MODIS snow cover product

The 8-day composite snow product MOD10A2 ranging from 2001 to 2014 was used for this study. They are available from the National Snow and Ice Data Center (NSIDC, <http://nsidc.org/NASA/MODIS>). The spatial resolution of MOD10A2 is 500 m, and a sinusoidal grid tiling system is used. The MOD10A2 8-day product is synthesized by the daily snow data MOD10A1 using a maximum time synthesis algorithm, which means that a pixel of a MOD10A2 image is determined as snow if the pixel is snow in any of the 8 daily MOD10A1 images. The MODIS 8-day snow product used in this study ranges from January 2001 to December 2014, 46 scenes each year, 640 scenes in total (4 scenes are missing: 2001.06.17, 2001.06.25, 2002.03.21, 2008.04.22).

Lots of previous studies have been carried out to validate the accuracy of MODIS snow products in different areas (Ault *et al.*, 2006; Liang *et al.*, 2008; Marchane *et al.*, 2015; Raleigh *et al.*, 2013; Wang *et al.*, 2008). In northern Xinjiang, China, Huang *et al.* (2007) has evaluated the snow cover identification accuracy of MOD10A1 and MOD10A2 by combining with measured data of local stations, and the results showed that MOD10A1 has the best identification accuracy of 58.2% under clear sky conditions, while MOD10A2 can effectively eliminate the influence of clouds and improve the snow classification accuracy, with a mean snow identification accuracy of 87.5%. Klein and Barnett (2003) compared MODIS

daily (MOD10A1) with operational snow cover maps produced by the National Operational Hydrologic Remote Sensing Center (NOHRSC) and against *in situ* Snowpack Telemetry (SNOTEL) measurements for the 2000–2001 snow season and found the agreement between the MODIS and NOHRSC snow maps was high with an overall agreement of 86%. An evaluation of MODIS daily (MOD10A1) and 8-day (MOD10A2) snow product by Zhou *et al.* (2005) in the Upper Rio Grande River Basin of United States using stream flow and SNOTEL measurements as a ground truth has indicated that MOD10A1 is susceptible to cloud interference and has higher omission errors of misclassifying snow as clouds, while the MODIS 8-day product has higher snow classification accuracy, improvement in suppressing clouds is apparent, and MOD10A2 can be more useful in evaluating the streamflow response to snow cover area changes considering its lower temporal resolutions and higher snow identification accuracy.

(2) Digital elevation models

The digital elevation model (DEM) used in this study is the Shuttle Radar Topography Mission (SRTM) data, with a resolution of 90 m. The SRTM data is freely available from: <http://srtm.csi.cgiar.org/SELECTION/inputCoord.asp>. The DEM is resampled at a 500-m resolution to match the MODIS snow data.

(3) *In situ* data

In this study, the daily average temperature from 2001 to 2012 recorded at three hydrological stations was used to verify the applicability of the MODIS land surface temperature data (MOD11A2) for the study area. Table 1 shows the information of the stations.

Table 1 The information of the three hydrological stations

Station	Full name	Longitude/Latitude	Elevation (m)
KSWT	Kensiwater	85°57'19"E/43°58'14"N	860
MY	Meiyao	85°51'49"E/43°54'34"N	1046
QSHZ	Qingshuihezi	86°3'42"E/43°54'53"N	1256

(4) MODIS LST product

We also used the MODIS 8-day global land surface temperature data (MOD11A2) to analyze spatial correlation between snow cover variability and temperature change. The MOD11A2 is composed from the MODIS daily LST data MOD11A1, and stored on a 1-km sinusoidal grid as the average values of clear-sky LSTs during an 8-day period. In order to verify if the MODIS product MOD11A2 is applicable to our study area, we conducted a regression analysis of the MOD11A2 data with *in situ* temperature observed at the stations (a total of 1656 pairs of data). Figure 2 shows the

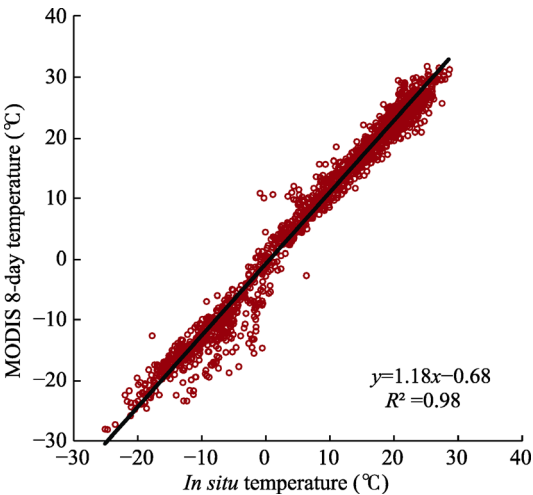


Figure 2 The relation between MOD11A2 LST data and *in situ* temperature of KSWT, MY and QSHZ

results of the MODIS 8-day temperature versus point measurement at the KSWT, MY and QSHZ stations and we found that the correlation coefficient is as high as 0.99 and $R^2 = 0.98$, which means the MOD11A2 LST data can fully meet the needs of this study.

3.2 Methods

The study focuses on the vertical distribution of snow cover and its relation with temperature, including vertical distribution of SAE during different months, annual change of SAE in different altitude zones, vertical distribution of annual snow cover days (SCDs), vertical distribution of long-term change of SCDs, and their relations with temperature. To accomplish the tasks, a zonation analysis was adopted, e.g. a series of altitude belts were created, some snow cover indices such as SAE and SCDs in each belt were calculated. The snow cover indices were estimated using the following formulas.

(1) Calculation of SAE and SCDs

The SAE is calculated by dividing the number of snow pixels within a specific range by the total number of pixels within the study area. The SCDs of a certain pixel are the total days that the pixel is covered by snow within a year. The SCDs reflect the snow cover duration of each pixel in a certain time interval and the SCDs of each pixel are calculated by using the following equation:

$$SCDs = 8 \times \sum_{i=1}^{46} is_snow(i) \quad (1)$$

where $is_snow(i) = 1$ indicates that the pixel is covered by snow and $is_snow(i) = 0$ indicates the pixel is not covered by snow; 46 is the total number of the MODIS 8-day images that cover the pixel within a year.

(2) Calculation of long-term change of SCDs

When calculating SCDs for a given year, there are two ways to define a year: a calendar year from January to December or a snow year from August of a calendar year to July of the next calendar year. The second one is a complete snow accumulation and ablation period. In order to make comparisons between the long-term trend of SCDs and winter temperature (from December to February of the next year), we adopted the second definition. The long-term change of SCDs from 2002 to 2014 for each pixel is calculated with the least-square linear fitting method. The formula is as follows (Wang *et al.*, 2015):

$$c = \frac{13 \times \sum_{i=1}^{13} i \times SCD_{i,jk} - \sum_{i=1}^{13} i \times \sum_{i=1}^{13} SCD_{i,jk}}{13 \times \sum_{i=1}^{13} i^2 - \left(\sum_{i=1}^{13} i \right)^2} \times 12 \quad (2)$$

where c is the specific number of days that has changed for each pixel from 2002 to 2014; i is the serial number from 1 to 13 representing the years from 2002 to 2014; $SCD_{i,jk}$ is the snow cover days of the pixel (j th row and k th column) in the i th year; the multiplier 12 is the number of years spanned. $c > 0$ indicates the SCDs for the pixel has increased for the past 13 years and $c < 0$ indicates SCDs has decreased and $c = 0$ indicates no change in SCDs.

4 Results and discussion

4.1 Vertical distribution of snow cover

The vertical distribution of SAE of each year was analyzed. Figure 3 shows the average SAE variation with the increase of elevation in each month. The SAE in each altitudinal range (every 100 m) of every month is the average value derived from the 8-day MODIS snow data in each month of all the 14 years (2001–2014), the weight was determined by the number of spanning days of the MODIS snow data in each of the same month. From features of each monthly SAE versus elevation, we divided the whole basin into five elevation zones (Zone A: <1100 m, Zone B: 1100–2100 m, Zone C: 2100–3200 m, Zone D: 3200–4000 m, and Zone E: > 4000 m), each zone has its own characteristics (see below). We also found that the variations of SAE with elevation have four different seasonal patterns, and each pattern shows common key characteristics of snow accumulation and ablation. Meanwhile, for each pattern, the vertical distribution curves show different characteristics at different elevation zones.

Pattern I, represented by curves in blue from December to February of the next year (winter months), has the following characteristics: (1) the SAE percentages of these months had no significant variation in Zone A, and snow covered 80%–95% of the zone. (2) The SAE percentages dropped rapidly from about 95% to below 40% in Zone B, but remained almost constant in Zone C and then increased with elevation in Zone D. (3) In Zone E, the increasing trends of SAE percentages with elevation had disappeared, and to the contrary there were downward trends in areas above 4400 m. Overall, the SAE percentages during December to February were much larger than other months (April to November) below 3200 m, but smaller in the higher altitude area (> 4500 m).

Pattern II, represented by the curves in red from May to September (summer months), has the following characteristics: (1) over the whole range of elevation, the SAE percentage showed a general increase with increasing elevation. (2) Zone A was snow free during these months. However, the SAE percentages started to increase in Zone B with elevation and the increasing rates in Zones B and C were insignificant, but the SAE percentages increased rapidly in Zones D and E, close to 100% above 4700 m. (3) In Zones B–E, the SAE decreased from May to July and increased again from July to September.

Pattern III is represented by the green dotted curves of March and November. Both curves are similar to those of the winter months especially in Zones C–E, but there are also some differences: (1) these two months were characterized by large changes in SAE due to accumulation (November) and ablation (March) in lower areas (Zones A and B). (2) Within Zone E, the SAE percentages were higher than the winter months. SAE decreased all the way from November to February of the next year and it increased rapidly from February to May, indicating the snowfall in Zone E mainly occurred in March and April. Overall, the SAE percentage showed an increase with elevation in Zone A, a decrease in Zones B and C, an increase in Zone D, and a rapid increase in Zone E.

Pattern IV is represented by the purple dotted curves of April and October. Both curves are similar to those of the summer months especially in Zones D and E, but there are also some characteristics: (1) the SAE percentages increased slowly in Zone A but faster in Zone B with elevation. (2) In Zone C, the curve patterns of these two months were similar to March and November and the winter months, but SAE was lower than those months. (3)

Within Zones D and E, the SAE curve patterns of both months were similar to the summer months. The SAE of the two months increased rapidly with elevation probably because of enhanced snowfall at higher mountainous areas.

The effects of altitude (elevation) on monthly snow cover can also be observed in Figure 3: (1) the monthly SAE in any month from October to April of the next year was sensitive to elevation in areas <2100 m (Zones A and B) and of elevation >3200 m (Zones D and E); (2) the monthly SAE in any month of May to September was very sensitive to elevation in area >3200 m (Zones D and E); and (3) area with elevation between 2100 m and 3200 m (Zone C) had the least variation in SAE with elevation change compared to the other zones.

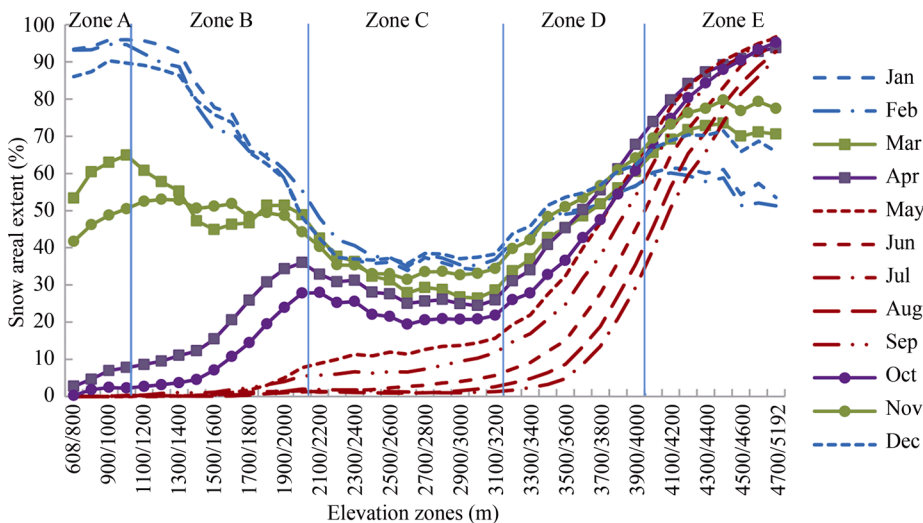


Figure 3 Vertical distribution of zone-averaged SAE in different months

4.2 The annual change of snow cover in five elevation zones

The annual change of SAE in the five elevation zones is shown in Figure 4. The SAE value

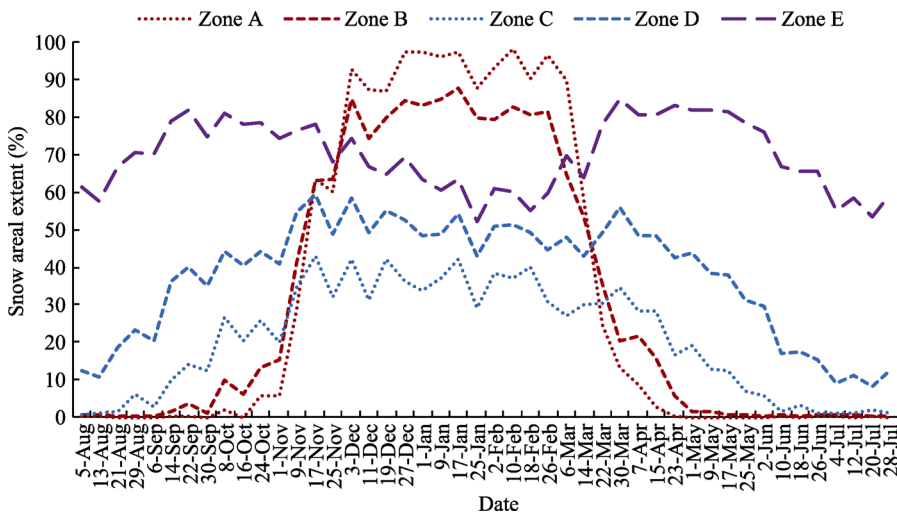


Figure 4 Annual change of SAE percentage in different elevation zones

is the average value from 2001 to 2014. It can be seen from Figure 4 that the SAE changes in the five zones show a common feature: accumulation in autumn and winter, and ablation in spring and summer. But each zone shows its own characteristics.

(1) The changes of SAE within Zones A and B were significant during the year. From December to February of the next year, the values of SAE were around 90% in Zone A and 80% in Zone B, which were much larger than the other three zones of higher elevations. March to May was the rapid snow ablation phase for both zones. From late May to October, the values of SAE were almost zero. In November there was a period of rapid increase in snow cover with the occurrence of seasonal snowfall within both zones.

(2) The SAE for Zone C was lower than 43% throughout the year and close to zero from July to mid-August. From mid-November to mid-March, the SAE varied between 29% and 43% and was the lowest among all the five zones. From mid-August to mid-November was a period of slow snow-accumulation and from mid-March to June was a period of slow snow-ablation.

(3) The variation of SAE in Zone D is similar to that in Zone C. Since the snowline elevation of the basin is within Zone D, the minimum SAE of this zone was around 10% and occurred in July. The snow accumulation and ablation periods of this zone were from mid-August to mid-November and April to June, respectively.

(4) In Zone E, the SAE was higher than 50% through the whole year. There were two periods with lower SAE in this zone: one was from July to August and the other was from December to February. The first one was because that the temperature from July to August in this zone was above 0 °C and snow ablation occurred during this period. The reasons for the second one can be twofold: the temperature inversion layer which appeared in winter months had an inhibiting effect for the snowfall in high elevation area; the wind blowing effect at high elevation zones may have contributed to snow cover decrease in winter.

4.3 Distribution of snow cover days

The distribution of the average SCDs from 2001 to 2014 is shown in Figure 5a. The basin can be cataloged into stable snow cover area and unstable snow cover area according to snow cover days. The threshold of SCDs used for separating stable from unstable snow cover areas is 60 days (2 months). The unstable snow cover area (< 60 days) is further divided into two subareas: the annual periodic unstable snow cover area in which snow appears every year and the SCDs is between 10–60 days and the non-cyclical unstable snow cover area in which snow appears only in some of the years and the SCDs is below 10 days. As shown in Figure 5a, the non-cyclical unstable snow cover area was mainly distributed along the Manasi River in the south central basin with an average elevation of 2717 m. It only accounted for about 2.7% of the whole basin. The annual periodic unstable snow cover area was located in the valleys of the upper reaches of the river. It accounted for about 13.7% of the basin area. While in the downstream region of the basin, the SCDs was generally 60–240 days, and the average elevation was relatively lower than the unstable snow cover area. The area with SCDs longer than 8 months occurred mainly in the mountainous regions of high elevation in the southwest, south, and central east of the basin, which accounted for about 34.4% of the area of the entire basin.

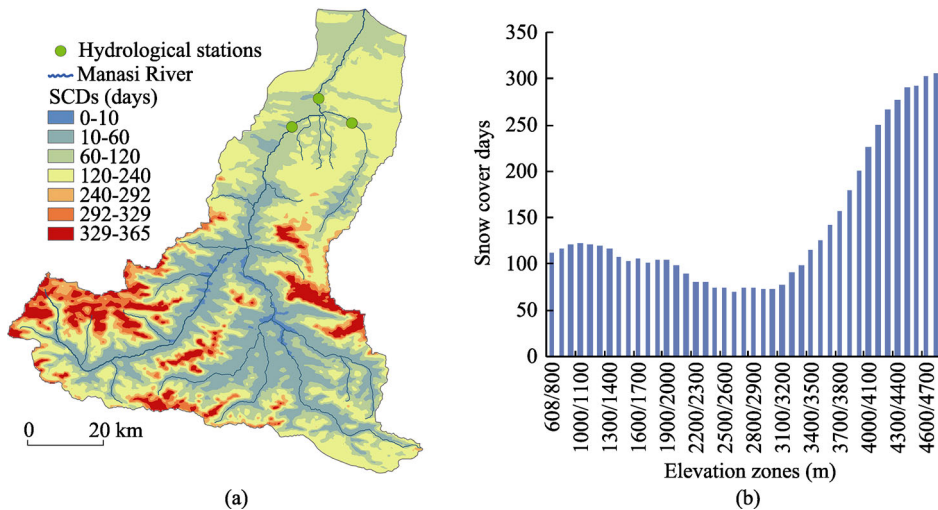


Figure 5 Horizontal (a) and vertical (b) distributions of average SCDs (from 2001 to 2014)

The vertical distribution of the average SCDs is shown in Figure 5b. We can see that the SCDs did not always increase with elevation. In the area above 3000 m, the SCDs increased with elevation. While in the area between the elevations of 1000 m and 3000 m, the SCDs showed a decrease with increasing elevation, which may be attributed to the temperature inversion in winter (see details in the next section) and different vertical distributions of SAE in all seasons.

4.4 Distribution of long-term change of snow cover days

The long-term change of SCDs from 2002 to 2014 for each pixel was calculated using Equation (2). The horizontal distribution of the SCDs changes displayed in Figure 6a indicates that 40.3% of the area showed negative changes in SCDs, and 12.1% of the area manifested a decrease of more than 18 days. The area with decreasing SCDs was mainly located in the southern mountainous region above 3600 m and that below 650 m in elevation. The SCDs for the remaining 59.7% of the pixels had positive changes and 11.4% of those showed an increase of more than 24 days in the past 13 years. The area with increased SCDs mainly occurred below 3600 m.

The vertical distribution of the SCDs changes is shown in Figure 6b. We can see that the change in SCDs showed a decreasing trend above 3600 m, while it showed an increasing trend below the elevation. The maximum increase happened in the area with elevations between 1600–1700 m.

4.5 The vertical relations between snow cover and temperature

The vertical distribution of the average MODIS 8-day temperature in different months from 2001 to 2014 was calculated and shown in Figure 7. The temperature is the average value of the daytime and nighttime temperature. It can be observed clearly from Figure 7 that a temperature inversion has occurred in winter (December to February) within Zone B, which is the most significant characteristic. In the northern side of the Tianshan Mountains, there was a

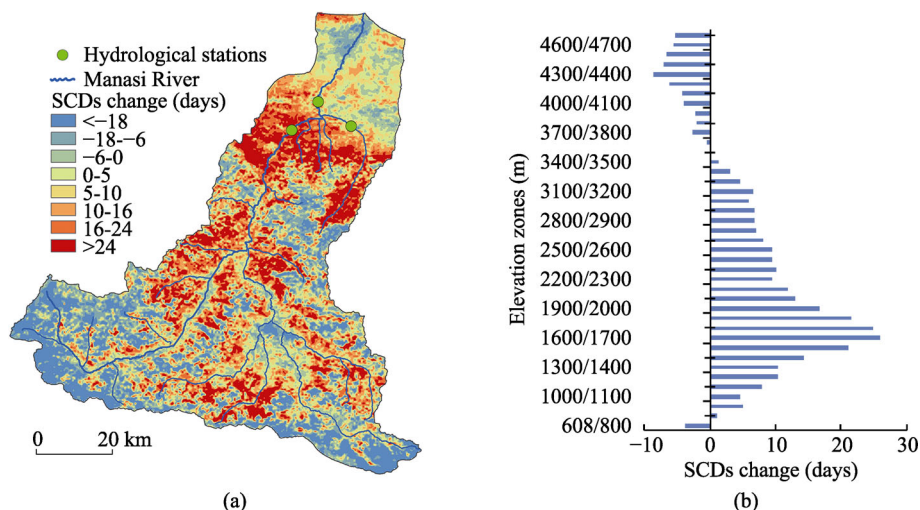


Figure 6 Horizontal (a) and vertical (b) distributions of long-term change in SCDs

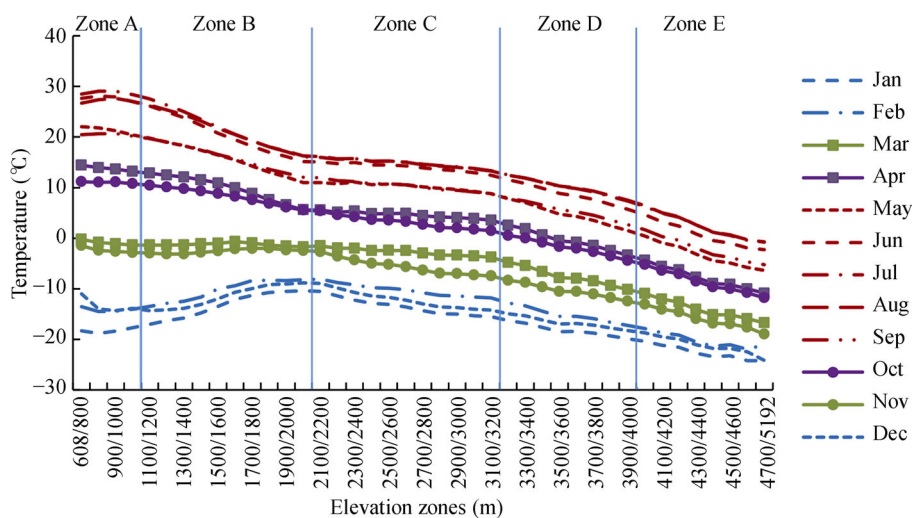


Figure 7 Vertical distribution of zone-averaged temperature in different months

temperature inversion layer at the altitude around 1500 m in winter. In the low-lying areas, cold air flowed along the slope into the low-lying valley, warm air was lifted and the movement of cold air was blocked by the terrain, a “cold air lake” formed at the bottom (Hu, 2004). The vertical distribution of the monthly averaged temperature can also be described in four patterns that are well correspondent to the SAE patterns, indicating a strong relationship between SAE and temperature (see Figure 3). The relations can be described as follows.

(1) During the winter months, the temperature inversion phenomenon played an important role in the distribution of snow cover in different zones. The average temperature in Zone A was about 5°C lower than that in Zone B, and it was much easier to form snowfall in Zone A. Therefore, the SAE percentage in the zone was much higher than the other zones. But in

Zone B, SAE decreased rapidly with increasing temperature and elevation. This coincidence indicates that the temperature inversion may have reduced SAE possibly due to less snowfall from the inversion layer, since the temperature was still negative. Also, little snowfall in Zones C and D led to a slow increase in SAE with increasing elevation. The SAE even showed a decrease probably due to wind blowing effect in Zone E (Hu, 2004). While during summer months (from May to September), the situation was much simpler. The temperature decreased with increasing elevation in all zones, and SAE increased within the whole elevation range correspondingly.

(2) February to April and October to December were two transitional periods. For February to April, land surface temperature rose rapidly from below -10°C to above $+10^{\circ}\text{C}$ in Zones A and B. Although the average temperature of March was near the melting point, March experienced a large reduction in SAE; from October to December, land surface temperature dropped rapidly from above 5°C to below -9°C . The average temperature of November was below or near the freezing point, but November experienced the large increase in SAE due to snow accumulation. However, in Zones C and E, the temperature in March and November was below 0°C , and the pattern of the SAE curve with increasing elevation is similar to the winter months.

(3) Judging from the regression analysis between the SAE percentage and temperature in vertical distribution for each month (Table 2), the correlations were all correspondent to the SAE and temperature patterns: the correlation between SAE and temperature from April to October was the most significant and that from December to February was the least. During the ablation period from April to July, the correlation in April was the most significant while from April to July, the significance decreased month-by-month. When snow accumulation began, the significance increased month-by-month from August to October. The poor correlation between snow cover and temperature in November to February was mainly caused by more snowfall in lower altitude area, wind blowing effect at high elevation zones and temperature inversion phenomenon. During a transitional period, the correlation in March and November improved considerably.

Table 2 Correlation coefficients between SAE and temperature on vertical distribution

Jan	Feb	Mar	Apr	May	Jun	Jul	Aug	Sep	Oct	Nov	Dec
-0.19	-0.10	-0.60	-0.97	-0.94	-0.85	-0.79	-0.82	-0.91	-0.96	-0.74	-0.24

4.6 The annual relations between SAE and temperature in five elevation zones

Figure 8 shows the annual changes of the 8-day average temperature of the past 14 years in the five different elevation zones. The 8-day average temperature derived from the MODIS 8-day temperature data product is the average value of all pixels in each zone. The change of temperature in different elevation zones showed a certain correspondence to that of the SAE presented in Figure 4.

In order to explore the relationship between the snow cover and land surface temperature, we performed a regression analysis between the 8-day SAE and temperature from 2001 to 2014 in the five elevation zones. The correlation coefficients are listed in Table 3. The

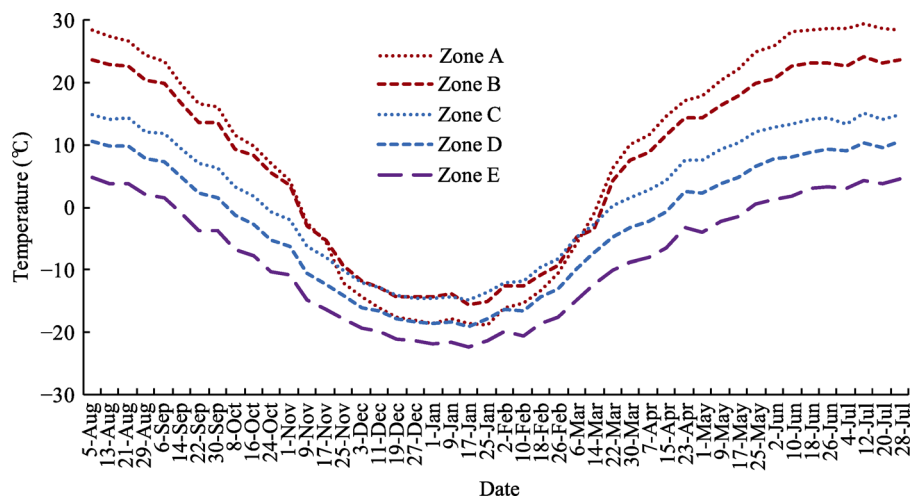


Figure 8 Annual change of temperature in the five elevation zones

correlation between the SAE and temperature decreased with increasing elevation. The correlation coefficient in the area below 2100 m (Zones A and B) was -0.82 to -0.93 , it decreased to 0.05 in the area above 4000 m (Zone E). The negative correlation between the SAE and temperature was significant in Zones A-D, but not significant in Zone E, which indicated that below a certain altitude, temperature was a key factor controlling the distribution of SAE. This result is consistent with those obtained by Beniston (2012), Morán-Tejeda *et al.* (2013), and Bi *et al.* (2015). Beniston (2012) found a threshold altitude at approximately 1500–2000 m in the European Alps. Morán-Tejeda *et al.* (2013) reported a threshold altitude of ~ 1400 m in Switzerland, and Bi *et al.* (2015) identified a threshold altitude of 3650 ± 150 m in the Heihe River Basin, an arid area of Western China. Those studies found that temperature is the primary controlling factor on SAE below the threshold altitude, while precipitation is the primary controlling factor on SAE above the threshold altitude.

Table 3 Correlation coefficients between SAE and temperature over annual variation

Year	Zone A	Zone B	Zone C	Zone D	Zone E
2001	−0.90	−0.92	−0.68	−0.54	0.23
2002	−0.90	−0.89	−0.71	−0.60	0.05
2003	−0.86	−0.90	−0.59	−0.52	0.24
2004	−0.89	−0.84	−0.77	−0.72	0.03
2005	−0.90	−0.90	−0.77	−0.74	−0.11
2006	−0.89	−0.90	−0.88	−0.84	−0.22
2007	−0.90	−0.90	−0.71	−0.71	−0.19
2008	−0.86	−0.86	−0.67	−0.64	0.07
2009	−0.91	−0.91	−0.40	−0.32	0.27
2010	−0.88	−0.88	−0.67	−0.67	−0.15
2011	−0.85	−0.88	−0.62	−0.67	0.04
2012	−0.90	−0.93	−0.69	−0.53	0.26
2013	−0.89	−0.92	−0.71	−0.69	−0.14
2014	−0.82	−0.92	−0.66	−0.56	0.26
Average	−0.88	−0.89	−0.68	−0.63	0.05

4.7 The vertical relations between long-term changes of SCDs and temperature

The long-term changes of temperatures of both winter and summer from 2002 to 2014 in each elevation zone are shown in Figure 9, the elevation range of each zone is 100 m. The value of temperature change in each zone is the average of all pixels of the zone. From this figure it can be seen that the summer temperature increased, while on the contrary the winter temperature showed a decreasing trend. This resulted in warmer summer and colder winter, suggesting an enlarged extent of temperature variation within a year. The vertical distribution curve of long-term changes of SCDs shown in Figure 6b and winter temperature had inverse shapes for the area below 3600 m, with correlation coefficient of -0.84 . The maximum amplitudes of SCDs and winter temperature changes were well correspondent to each other. The change in snow cover in the area below 3600 m was seasonal, which appeared mostly in winter, so it was affected mainly by winter temperature. While in the area above 3600 m, the correlation between SCDs and winter temperature change was poor. The change of SCDs above 3600 m was negative, probably because that the summer temperature increased over the whole basin, which might lead to the decrease in SCDs in the area.

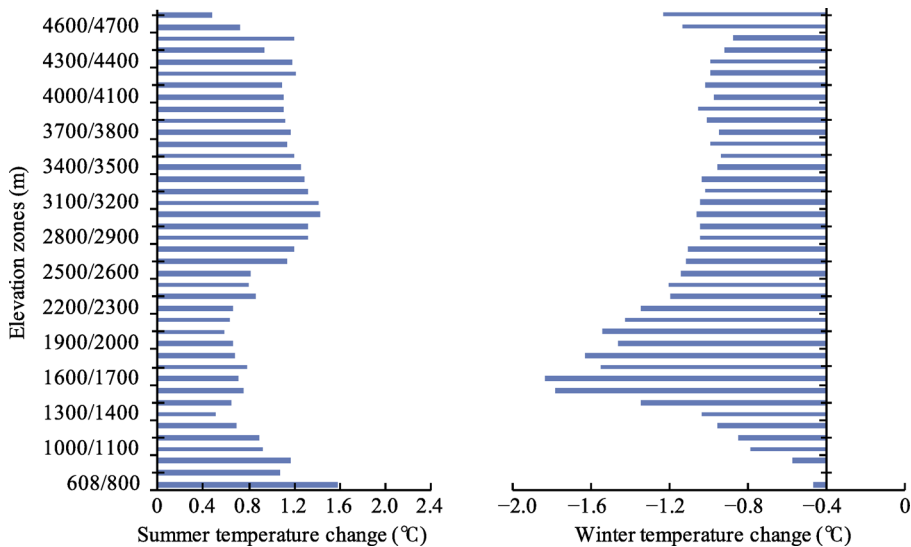


Figure 9 Vertical distributions of long-term changes of summer and winter temperatures

4.8 Other factors affecting snow cover change

It is well known that SAE is affected by both temperature and precipitation, snowfall contributes significantly to snow cover variation, while temperature rise (and subsequent melting) is the principal impact factor during warm season (Bavay *et al.*, 2013; Wang *et al.*, 2015; Liu *et al.*, 2007). This study mainly investigated the vertical change of snow cover and its relation with elevation and temperature. The results show that the most significant negative correlation between SAE and temperature occurred during April to October and in Zones A-D, and the least correlation occurred during December to February and in Zone E. The poor correlation between SAE and temperature during winter and in Zone E may indicate that other factors such as precipitation, wind blowing, sublimation, etc. might have played

important roles. Precipitation is the principal factor affecting SAE in high altitude area (Beniston, 2012; Morán-Tejeda *et al.*, 2013), high-speed wind can also blow the snow away and change the distribution of snow cover in the local area (Li *et al.*, 2014), sublimation recognized as an important hydrological process in high altitude regions would be another reason for the SAE decrease in winter season (Li *et al.*, 2009; Bi *et al.*, 2015). Unfortunately, there was no observed sublimation and wind data in the basin, and precipitation data obtained from the three hydrological stations located at low elevation areas may not represent the precipitation at high altitude regions. The TRMM (Tropical Rainfall Measuring Mission) rainfall data maybe a promising source of precipitation data for further study after correction and being down scaled. All these demonstrate that identification of the main factors that control snow cover in high elevation areas is still challenging due to lack of observation data and thus deserves further investigation.

5 Conclusions

Based on refined zonation analysis of the MODIS 8-day composite snow data products MOD10A2, MODIS land surface temperature data, and *in situ* daily temperature, the spatio-temporal variation of snow cover and its relation with temperature in Manasi River Basin were investigated at various characteristic elevation zones in this study. We concluded that:

(1) The vertical distribution of SAE indicates four different patterns in a year, each pattern has different features at different altitudes and is well correspondent to patterns of temperature variation. The SAE and temperature have a good vertical relationship in all seasons except for winter. The poor relationship in winter is possibly attributed to the more snowfall in lower altitude region, wind blowing effect at high elevation zones and temperature inversion phenomenon.

(2) The monthly SAE in any month from October to April of the next year is sensitive to elevation in regions of elevation < 2100 m and of elevation > 3200 m, the monthly SAE in any month of May to September is very sensitive to elevation in area of elevation > 3200 m, area of elevation between 2100–3200 m has the least variation in SAE with elevation change compared to the other regions.

(3) The annual changes in SAE in each altitudinal zone show distinct seasonal characteristics. The correlation between SAE and temperature decreases with increasing elevation. The negative correlation is significant in area below 4000 m, but not significant in area above 4000 m.

(4) The average distribution of SCDs during the period 2001–2014 shows distinct vertical variations. The average SCDs increase with increasing elevation except for the area between 1000 m and 3000 m in elevation, where the SCDs decrease with increasing altitude, which may be attributed to the temperature inversion in winter and different vertical distributions of SAE in all seasons.

(5) The long-term changes in winter temperature are negative, while changes in summer temperature are positive during 2002–2014. The increasing trend of SCDs has a strong correlation with the decreasing trend of winter temperature in the area below 3600 m, and the decreasing trend of SCDs is attributed to the increasing trend of summer temperature in the area above 3600 m.

References

- Ault T W, Czajkowski K P, Benko T *et al.*, 2006. Validation of the MODIS snow product and cloud mask using student and NWS cooperative station observations in the Lower Great Lakes Region. *Remote Sensing of Environment*, 105: 341–353.
- Barnett T P, Dumenil L, Schlese U *et al.*, 1989. The effect of Eurasian snow cover on regional and global climate variations. *Journal of the Atmospheric Sciences*, 46: 661–685.
- Bavay M, Grünwald T, Lehning M, 2013. Response of snow cover and runoff to climate change in high alpine catchments of eastern Switzerland. *Advances in Water Resources*, 55: 4–16.
- Beniston M, 2012. Is snow in the Alps receding or disappearing? *WIREs Climate Change*, 3: 349–358.
- Bi Y B, Xie H J, Huang C L *et al.*, 2015. Snow cover variations and controlling factors at upper Heihe River Basin, northwestern China. *Remote Sensing*, 7: 6741–6762.
- Bosilovich M G, 2006. A comparison of MODIS land surface temperature with *in situ* observations. *Geophysical Research Letters*, 33: L20112.
- Brown R D, Robinson D A, 2011. Northern Hemisphere spring snow cover variability and change over 1922–2010 including an assessment of uncertainty. *Cryosphere*, 5: 219–229.
- Coll C, Wan Z, Galve J M, 2009. Temperature-based and radiance-based validations of the V5 MODIS land surface temperature product. *Journal of Geophysical Research-Atmospheres*, 114: D20102.
- Dietz A J, Kuenzer C, Dech S, 2015. Global Snow Pack: A new set of snow cover parameters for studying status and dynamics of the planetary snow cover extent. *Remote Sensing Letters*, 6: 844–853.
- Feng X Z, Li W J, Shi Z T *et al.*, 2000. Satellite snowcover monitoring and snowmelt runoff simulation of Manas River in Tianshan Region. *Remote Sensing Technology and Application*, 15: 18–21. (in Chinese)
- Hall D K, 1988. Assessment of polar climate change using satellite technology. *Reviews of Geophysics*, 26: 26–39.
- Hu R, 2004. Physical Geography of the Tianshan Mountains in China. Beijing: China Environmental Science Press, 443pp. (in Chinese)
- Huang X, Zhang X, Li X *et al.*, 2007. Accuracy analysis for MODIS snow products of MOD10A1 and MOD10A2 in northern Xinjiang area. *Journal of Glaciology and Geocryology*, 29: 722–729. (in Chinese)
- Hulley G C, Hook S J, 2009. Intercomparison of versions 4, 4.1 and 5 of the MODIS land surface temperature and emissivity products and validation with laboratory measurements of sand samples from the Namib Desert, Namibia. *Remote Sensing of Environment*, 113: 1313–1318.
- Jin X, Ke C Q, Xu Y Y *et al.*, 2015. Spatial and temporal variations of snow cover in the Loess Plateau, China. *International Journal of Climatology*, 35: 1721–1731.
- Klein A G, Barnett A C, 2003. Validation of daily MODIS snow cover maps of the upper Rio Grande River Basin for the 2000–2001 snow year. *Remote Sensing of Environment*, 86: 162–176.
- Li H, Wang J, Bai Y *et al.*, 2009. The snow hydrological processes during a representative snow cover period in Binggou Watershed in the upper reaches of Heihe River. *Journal of Glaciology and Geocryology*, 31: 294–300. (in Chinese)
- Li H, Wang J, Hao X, 2014. Role of blowing snow in snow processes in Qilian mountainous region. *Sciences in Cold and Arid Regions*, 6: 124–130.
- Liang T G, Huang X D, Wu C X *et al.*, 2008. An application of MODIS data to snow cover monitoring in a pastoral area: A case study in northern Xinjiang, China. *Remote Sensing of Environment*, 112: 1514–1526.
- Liu G, Wu R, Zhang Y *et al.*, 2014. The summer snow cover anomaly over the Tibetan Plateau and its association with simultaneous precipitation over the mei-yu-baiu region. *Advances in Atmospheric Sciences*, 31: 755–764.
- Liu J, Yang J, Chen R, 2007. Annual variations of snow cover and its relation to air temperature and precipitation in Dongkemadi River Basin in the source regions of the Yangtze River. *Journal of Glaciology and Geocryology*, 29: 862–868. (in Chinese)
- Marchane A, Jarlan L, Hanich L *et al.*, 2015. Assessment of daily MODIS snow cover products to monitor snow cover dynamics over the Moroccan Atlas mountain range. *Remote Sensing of Environment*, 160: 72–86.

- Mishra B, Babel M S, Tripathi N K, 2013. Analysis of climatic variability and snow cover in the Kaligandaki River Basin, Himalaya, Nepal. *Theoretical and Applied Climatology*, 116: 681–694.
- Morán-Tejeda E, López-Moreno J I, Beniston M, 2013. The changing roles of temperature and precipitation on snowpack variability in Switzerland as a function of altitude. *Geophysical Research Letters*, 40: 2131–2136.
- Raleigh M S, Rittger K, Moore C E *et al.*, 2013. Ground-based testing of MODIS fractional snow cover in subalpine meadows and forests of the Sierra Nevada. *Remote Sensing of Environment*, 128: 44–57.
- She J, Zhang Y, Li X *et al.*, 2015. Spatial and temporal characteristics of snow cover in the Tizinafu Watershed of the Western Kunlun Mountains. *Remote Sensing*, 7: 3426–3445.
- Spiess M, Maussion F, Möller M *et al.*, 2015. MODIS derived equilibrium line altitude estimates for Purogangri Ice Cap, Tibetan Plateau, and their relation to climatic predictors (2001–2012). *Geografiska Annaler: Series A, Physical Geography*, 97: 599–614.
- Szczypta C, Gascoin S, Houet T *et al.*, 2015. Impact of climate and land cover changes on snow cover in a small Pyrenean catchment. *Journal of Hydrology*, 521: 84–99.
- Tahir A A, Chevallier P, Arnaud Y *et al.*, 2015. Snow cover trend and hydrological characteristics of the Astore River basin (Western Himalayas) and its comparison to the Hunza basin (Karakoram region). *The Science of the Total Environment*, 505: 748–761.
- Tang Z, Wang J, Li H *et al.*, 2013. Spatiotemporal changes of snow cover over the Tibetan Plateau based on cloud-removed moderate resolution imaging spectroradiometer fractional snow cover product from 2001 to 2011. *Journal of Applied Remote Sensing*, 7: 073582.
- Wan Z, 2008. New refinements and validation of the MODIS land-surface temperature/emissivity products. *Remote Sensing of Environment*, 112: 59–74.
- Wang W, Huang X, Deng J *et al.*, 2015. Spatio-temporal change of snow cover and its response to climate over the Tibetan Plateau based on an improved daily cloud-free snow cover product. *Remote Sensing*, 7: 169–194.
- Wang X, Xie H, Liang T, 2008. Evaluation of MODIS snow cover and cloud mask and its application in northern Xinjiang, China. *Remote Sensing of Environment*, 112: 1497–1513.
- Wang X, Zheng H, Chen Y *et al.*, 2014. Mapping snow cover variations using a MODIS daily cloud-free snow cover product in Northeast China. *Journal of Applied Remote Sensing*, 8: 084681.
- Yang C, Zhao Z, Ni J *et al.*, 2012. Temporal and spatial analysis of changes in snow cover in western Sichuan based on MODIS images. *Science China Earth Sciences*, 55: 1329–1335.
- Zhou X, Xie H, Hendrickx J M H, 2005. Statistical evaluation of remotely sensed snow-cover products with constraints from streamflow and SNOTEL measurements. *Remote Sensing of Environment*, 94: 214–231.